# Extreme Precipitation Events in the South Central United States During Spring 2010: Historical Perspective, Role of ENSO and Trends

by

R. W. Higgins[1], V. E. Kousky[2] and P. Xie[1]

[1]Climate Prediction Center, NOAA/NWS/NCEP, Camp Springs, MD, 20746

[2]WYLE Information Systems, Mclean, VA, 22102

November 2010

Submitted to Journal of Hydrometeorology

---

Corresponding author address: Dr. R. W. Higgins,
Director, Climate Prediction Center, NOAA/NWS/NCEP,
Washington, DC, 20233, USA

## Abstract

An analysis of extreme daily precipitation events that occurred in the South Central United States during spring 2010 is carried out using gridded station data and reanalysis products in use at the National Centers for Environmental Prediction (NCEP). Various aspects of the daily extremes are examined from a climate perspective using a 62 year (1948-2010) period of record, including their historical ranking, common circulation features, moisture plumes, and the possible influence of ENSO. The analysis includes a comparison to the daily extremes that occurred during the spring and summer of 1993, the year of the historic floods in the Midwest, and also considers how the frequency and intensity of daily extremes is changing in the United States.

It is shown that each of the spring 2010 flash flood events was associated with historic daily rainfall totals. While there were circulation features in common to several of the cases, a unique combination of synoptic-scale and mesoscale circulation features came together to define each case. Each case exhibited characteristics of the "Maya Express" flood events that link tropical moisture plumes from the Caribbean and Gulf of Mexico to mid-latitude flooding over the central United States. The heavy precipitation regime over the United States during the spring and summer of 2010 also exhibited a number of similarities to that during 1993, including a build-up phase during the spring with localized heavy rain events and flash flooding, and a sustained phase during the summer with heavy rain events and more generalized flooding over larger areas. Consistent with recent assessment reports, it is shown that extreme daily precipitation events in the United States have increased in every month of the year during the most recent 30 year period (1979-2009) when compared to the earlier period (1948-1978), though the increases are relatively small during the spring and summer months.

## 1.0 Introduction

The spring of 2010 was characterized by a large number of localized heavy rain events leading to flash flooding across portions of the South Central United States. For example, on May 3rd a heavy precipitation event in Nashville, Tennessee led to flooding that killed 31 people, which was the highest death toll from a non-tropical cyclone flooding event in the United States since 1994. On June 11th a heavy precipitation event that occurred in just a few hours over mountainous terrain in western Arkansas led to the disastrous flash flood in Albert Pike Recreation Area which killed 20 people. The period June 14-15, 2010 was the rainiest two-day period in history for Oklahoma City, which experienced heavy flooding and extensive damage, with rainfall totals exceeding 10 inches in some areas. Other historic extreme events were observed during May and June 2010 in locations that included eastern Texas and South Central Kansas. Subsequent to these spring extreme events, heavy rains continued across portions of the upper Midwest and northern Great Plains during July and August, including Iowa, Illinois, South Dakota and Minnesota.

With the large number of heavy precipitation events leading to major flooding during the spring of 2010, the NOAA / National Weather Service (NWS) received a "flood" of questions asking whether the events were related to climate change. Such questions are consistent with recent assessment reports (e.g. United States Global Change Research Program (USGCRP), 2009), that have concluded that precipitation falling in the heaviest downpours in the United States has increased approximately 20 percent on average in the past century, and that this trend is very likely to continue, with the largest increases in the wettest places. The USGCRP (2009) report goes on to say that widespread impacts (e.g. to the water, energy, transportation,

agriculture, ecosystems, and health sectors) are due to changes in the frequency and intensity of heavy precipitation events that are occurring now and that are expected to increase.

The NWS is responsible for providing early warning of weather and hydrologic extremes, as well as accurate information with minimal uncertainty on their possible causes. Improved attribution of the causes of these events supports the NWS mission requirements to help the public prepare for and respond to the associated flooding threats.

This paper addresses some of the questions people are asking about the spring 2010 precipitation and flooding events, but from a climate perspective:

*How did the spring 2010 precipitation events rank in the historical record?*

*Were there circulation features in common to these events?*

*How did these events compare with those that occurred during 1993?*

*Were these events influenced by ENSO?*

*How is the frequency and intensity of precipitation extremes changing?*

The questions above are examined using operational analyses produced by the National Centers for Environmental Prediction (NCEP), including the Climate Prediction Center (CPC) Unified global daily gauge analysis (1948-present), and the NCEP/NCAR 40 year (1957-1996) Reanalysis (Kalnay et al. 1996), and the Climate Data Assimilation System which continued the NCEP/NCAR Reanalysis forward in real time (1997-present).

This study is focused on the precipitation extremes that occurred during the spring of 2010, and not on the very wet conditions and more generalized flooding that occurred in the upper Midwest and northern Great Plains during the summer of 2010.

A brief summary of the data sets and analysis procedures (section 2) is followed by an examination of the historical rankings of the spring 2010 extreme precipitation events (section

3). Circulation patterns and moisture plumes associated with the events are examined in section 4. Comparisons of the 2010 extreme events to those that occurred during the historic 1993 Midwest flooding episode are considered in section 5. Relationships to the ENSO cycle and long term trends in precipitation extremes are discussed in sections 6 and 7, respectively. A summary and plans for future studies are discussed in section 8.

## 2.0 Data Sets and Analysis Procedure

### 2.1 Observed Precipitation

The observed daily precipitation analysis was obtained from the CPC Unified Raingauge Database (Chen et al. 2008; Higgins et al. 2000). The database averages roughly 17000 daily station reports around the globe, with excellent coverage over the United States (roughly 10000 daily station reports). The database was used to produce a multi-year (1948-present) daily precipitation analysis over the continental United States. The analysis is on a (latitude, longitude)=(0.125°, 0.125°) grid (approximate 14 km) and was produced using an Optimal Interpolation (OI) scheme. Precipitation was accumulated over a 24-hour period (12Z, 12Z) ending at 12Z on the target date. Several types of quality control were applied including "duplicate station" and "buddy" checks among others. Previous assessments of objective techniques for gauge-based analyses of daily precipitation (e.g. Chen et al. 2008) have shown that OI-based schemes are among the best over the complex terrain of the western US, though we acknowledge that our particular choice of analysis scheme is a source of uncertainty. Relationships between the spatial distribution and temporal continuity of the station data and errors in the final gridded OI analysis were examined in Chen et al. (2008).

### 2.2 NCEP/NCAR Reanalysis

Circulation features associated with the spring 2010 precipitation extremes were examined using the NCEP/NCAR 40-yr (1957-1996) reanalysis (Kalnay et al. 1996; hereafter referred to as R1) and the Climate Data Assimilation System (CDAS), which continued R1 forward in real time. R1 used a frozen state-of-the-art global data assimilation system and a database as complete as possible. The data assimilation and the model used were identical to the global system implemented operationally at NCEP in January 1995, except that the horizontal resolution was T62 (about 210 km). R1 was continued forward in real time using CDAS to allow reliable comparison of current anomalies with those in earlier decades (the primary application employed here). The CPC currently uses CDAS for real-time monitoring and forecast purposes. In this study we examine the following fields: 500-hPa height, 500-hPa vector wind, 500-hPa vertical motion, 925-hPa vector wind, sea-level pressure, and precipitable water. Results from R1 are based on daily averages, unless otherwise indicated. Anomalies in Fig. 7 are computed as departures from a 1971-2000 base period.

### 2.3 Data Processing

Historical rankings for each event were obtained using the observed daily precipitation analysis from the CPC Unified Raingauge Database (see section 2.1). Daily rainfall for the 15 day period centered on the target date (+/- 7 days) were ranked for each (latitude, longitude) = (0.125°, 0.125°) grid box for the 62-year period (1948-present). Rankings for the spring 2010 heavy precipitation events were obtained using the grid box surrounding the target location.

Other tests are performed in section 3, involving counting extremes at various daily precipitation thresholds over particular regions. The details of these procedures are discussed below as they are used.

## 3. Historical Ranking

Daily precipitation totals for five spring 2010 extreme events, each of which ranked first in the historical record at the location of interest are examined. The rankings for each event were derived from the CPC daily gauge precipitation analysis (1948-present; 12Z-12Z). In each case, the daily precipitation pattern is shown (Fig. 1) as well as the percentile rankings for daily precipitation amounts in the grid box surrounding the location of interest (Fig. 2). For reference, precipitation amounts for 99$^{th}$ percentile rankings are indicated by the horizontal dashed lines on Fig. 2. A summary of the results for all five events is also given in Table 1.

**Nashville, Tennessee:** The major flooding event at Nashville, Tennessee occurred on May 3, 2010 (Fig. 1a). Daily rainfall on May 3, for the grid box surrounding Nashville was 184.0 mm, which ranked first in the historical record (Fig. 2a).

**Eastern Texas:** The major flooding event in eastern Texas occurred on June 10, 2010 (Fig. 1b). Daily rainfall on June 10, for the grid box with the maximum rainfall in eastern Texas was 216.4 mm, which ranked first in the historical record (Fig. 2b).

**Western Arkansas:** The major flooding event in western Arkansas occurred on June 11, 2010 (Fig. 1c). Daily rainfall on June 11, for the grid box with the maximum rainfall in western Arkansas was 103.4 mm, which ranked first in the historical record (Fig. 2c).

**South Central Kansas:** The major flooding event in South Central Kansas occurred on June 13, 2010 (Fig. 1d). Daily rainfall on June 13, for the grid box with the maximum rainfall in south-central Kansas was 167.5 mm, which ranked first in the historical record (Fig. 2d).

**Central Oklahoma:** The major flooding event in Central Oklahoma occurred on June 15, 2010 (Fig. 1e). Daily rainfall on June 15, for the grid box with the maximum rainfall in central Oklahoma was 147.0 mm, which ranked first in the historical record (Fig. 2e).

The 5 extreme events highlighted here are a subset of the total number that occurred during May-June 2010, but they are representative of the precipitation regime that prevailed over the South Central United States during the period. For reference, if all grid boxes over the continental United States (hereafter CONUS) are considered, then the weather systems that occurred on these five dates (May 3, June 10, June 11, June 13, June 15) plus two adjacent dates (May 2 and June 12, on which the same weather systems were present) accounted for roughly half (48%) of the total number of grid boxes at which record daily rainfall was observed during the period May – June 2010.

Each of the selected daily precipitation extremes was associated with historical rainfall totals. Although May-June 2010 was exceptional in terms of the number of extreme rainfall and major flood events over that two month period, this does not confirm or deny a trend in these types of events (see Section 7).

### 3.1 Upper Bounds on Daily Precipitation Extremes

Spatial maps of the extreme maximum precipitation values that have occurred at each location are noisy (bulls-eyes) due to the insufficient length of the historical data record (1948-present). Although there are a number of events with similar characteristics in the historical record (i.e. precipitation amounts, moisture transport, etc.), they have occurred at different locations, so it becomes a sampling problem to characterize how unusual the spring 2010 events were. How long does the historical record have to be (100 years, 1000 years, etc.) in order to

capture all possible synoptic events? Clearly, a record length that is many times greater than the one currently available is required to ensure adequate sampling of extreme events.

For planning purposes we can estimate the upper bounds on daily precipitation extremes that could reasonably be expected to occur given a much longer historical record. A simple approach is to determine the extreme maximum value that has been observed in a specified region in the actual historical record and to use that value as an estimate of what might reasonably be expected to occur at all locations within the region, given a long enough historical record. Such an estimate will be sensitive to the size of the region, so a key consideration is to select regions of the appropriate size to help ensure that all locations are within roughly the same climate zones. Also, the estimates will depend on whether raw station data or gridded analyses are used to identify extreme events, as the former will yield larger values than the latter.

For the purposes of this exercise, the OI gridded daily analysis is used, in part because the gridded data have undergone rigorous quality control (see section 2.1). After some experimentation with the sensitivity of the upper bounds on daily precipitation extremes to the size of the region, grid boxes at a horizontal resolution of (latitude, longitude)=(1°x1°) were chosen. Each grid point (at 0.25° resolution) within the 1° grid box was checked, and spatial maps of the extreme maximum daily precipitation amount within the 1° box were generated by month (Fig. 3).

During the warm season the upper bounds can exceed 300 mm along the Gulf Coast (July-October) and the East Coast (August-September) due to land falling tropical cyclones, and (especially during October) due to other non-tropical triggering mechanisms including coastal extratropical cyclones, synoptic-scale fronts, topography and large-scale ascent (Nielsen-Gammon et al. 2005). The North American monsoon can provide rainfall exceeding 100 mm

per day over portions of the Southwest during August and September. Synoptic-scale disturbances can provide rainfall exceeding 200 mm per day along the Gulf Coast (November-March) and the West Coast (November- March). Moist plumes from the Gulf of Mexico and the Great Plains low-level jet contribute to extreme events exceeding 250 mm per day along the Gulf Coast and in portions of the Great Plains during the spring (April-June). Elsewhere, the upper bounds are generally in the range of 100-200 mm per day through much of the year, except over the intermountain west where they tend to be less than 75 mm per day.

**4. Circulation Patterns and Moisture Plumes**

The synoptic evolution of the spring 2010 heavy precipitation events is examined, with emphasis on the circulation features and associated moisture plumes. The following questions are addressed:

(i) Were there any circulation features in common to the spring 2010 events?

(ii) What was the role of moisture plumes from the Gulf of Mexico? Were they unprecedented (e.g. in terms of precipitable water)?

The large-scale and regional circulation patterns associated with each case were examined using R1 (Kalnay et al 1996). For the analysis the following fields are shown: 500-hPa height, 500-hPa vector wind, 925-hPa height, 925-hPa vector wind and precipitable water. The following fields were also examined (but are not shown): 500-hPa vertical motion and sea-level pressure. A brief summary of the results for all 5 events is given below with some emphasis on features in common to multiple cases:

**Nashville, Tennessee (May 3, 2010):** This case featured a strong upper-level trough over the central U.S., with a strong flow from the Rio Grande Valley northeastward across the

Tennessee and Ohio Valleys (Fig. 4, top). Strong low-level flow and moisture transport extended from the central Gulf of Mexico north-northeastward across the Southeast and Mid-Atlantic states (Fig. 4, bottom). The origins of this moisture plume extended farther south and east towards the Caribbean Sea in association with an active Caribbean easterly low-level jet (not shown). Moist (high precipitable water) air was clearly evident along the western edge of the subtropical ridge anchored off the southeastern coast of the United States. Large low-level moisture convergence and strong synoptic-scale upward motion were evident over the Tennessee and Ohio Valleys (not shown), and a cold front slowly moved from the Mississippi Valley to the Tennessee and Ohio Valleys (particularly apparent from comparison of 6-h analyses).

**Eastern Texas (June 10, 2010):** During this event an upper-level cut-off low over Northeast Texas, embedded within a synoptic-scale ridge, moved slowly northeastward (Fig. 4, top). Strong low-level flow and moisture transport from the western Gulf of Mexico progressed northward across eastern Texas (Fig. 4, bottom) . Low-level moisture convergence, weak upper-level flow, weak vertical wind shear, and relatively cold air (center of cut-off low) all favored the slow moving convective storms that characterized this event.

**Western Arkansas (June 11, 2010):** This case, a continuation of the previous, featured an upper-level trough over northwestern Arkansas embedded within a synoptic-scale ridge (Fig. 4, top). Strong low-level flow and moisture transport from the western Gulf of Mexico progressed northward across eastern Texas and Arkansas towards the upper Midwest (Fig. 4, bottom). Low-level moisture convergence, weak upper-level flow, and strong upward motion all favored the slow moving convective storms that characterized this event.

**South Central Kansas (June 13, 2010):** A strong upper-level trough over the western U.S. featured strong southwesterly flow from New Mexico northeastward across eastern Colorado

(Fig. 4, top). Strong low-level flow and moisture transport from the western Gulf of Mexico progressed north-northeastward across the southern and central Plains (Fig. 4, bottom). Large low-level moisture convergence occurred over southern Kansas. Low-level northerly flow over the Dakotas and Nebraska and low-level southerly flow over Texas and Oklahoma impinged on a slow-moving frontal boundary across Kansas, which provided lift for the warm moist low-level flow and favored organized slow moving convective storms and the training of convection.

**Central Oklahoma (June 15, 2010):** A weakening upper-level trough over the central Great Plains was embedded in broad west southwesterly flow from New Mexico eastward across the central U.S. (Fig. 4, top). Low-level flow and moisture transport from the western Gulf of Mexico progressed northward across Texas and into Oklahoma (Fig. 4e, bottom). Low-level moisture convergence and strong upward motion over north Texas and southern Oklahoma favored slow moving convective storms in the region, including Oklahoma City.

Each of the heavy precipitation and flooding events had features in common. All 5 cases were associated with warm moist air masses that brought record-breaking warm temperatures to surrounding regions of the country. During the overnight hours of the June 11$^{th}$ flood in Arkansas, fifty airports in the Southern and Midwestern United States experienced record warm minimum temperatures. Just prior to the Nashville, Tennessee flood on May 3$^{rd}$ , over 100 locations in the eastern half of the U.S. experienced record warm minimum temperatures on May 2$^{nd}$ . And the air mass that spawned the June 15$^{th}$ Oklahoma City floods set record warm minimum temperatures at more than 2 dozen airports across the central and Eastern portions of the U.S. on June 14$^{th}$ .

Several of the cases had circulation features in common. For example, the May 3$^{rd}$ Nashville and June 13$^{th}$ South Central Kansas cases had similar large-scale circulation patterns, but with

the Nashville pattern shifted to the east. The June 11th western Arkansas and June 15th Central Oklahoma cases both featured upper-level troughs, but the low-level circulation features were much stronger in the western Arkansas case. While there were other circulation features in common to several of the cases (e.g. slowly moving frontal boundaries and areas of strong upward motion), in general a unique combination of synoptic-scale and mesoscale circulation features came together to define each case. Successful forecasts of these events must capture all of these features as well as the subtle interplay between them.

All 5 cases featured strong low-level flow and moisture transport from the Gulf of Mexico northward into the southern Plains or Southeast. Spatial maps of precipitable water (PW) show the presence of these plumes of high PW air in the vicinity of (and to the east) of the major flood events (Fig. 5). In each case the moisture plumes in Fig. 5 extended deep into the Caribbean, and exhibited the characteristics of the "Maya Express" flood events (Dirmeyer and Kinter 2009) that link tropical moisture from the Caribbean and Gulf of Mexico to mid-latitude flooding over North America. During the heavy rainfall events the fetch of Caribbean moisture linked into the Great Plains low-level jet, creating a much longer "atmospheric river" of moisture. These cases were also related to strengthening or displacement of the Atlantic subtropical ridge, as was the case with the Maya Express events of Dirmeyer and Kinter (2009). It is worth noting that a link between moisture from the Caribbean Sea and the flooding over the Great Plains during 1993 has also been established in previous work (Dirmeyer and Brubaker, 1999).

The atmospheric PW associated with these events was also examined at specific locations near the extreme precipitation events to see whether the PW values were unprecedented. Moist air masses were present in each case, with PW values close to 50 mm, which is quite common for tropical air advancing northward from the Caribbean and Gulf of Mexico. Although the PW

values were high, they were not at record levels when compared to other events in the historical record. Extreme values over the US may reach 55-60 mm (and on rare occasions near 65 mm), associated with land-falling tropical cyclones. It is also worth noting that in the deep Tropics (Amazon Basin, Indonesia regions) PW values are often as high as 60-65mm. Nevertheless, the spring 2010 events over the U.S. were textbook examples of the association of heavy rainfall with strong moisture feeds and high PW air.

**5. Comparison to 1993**

In this section we provide a brief comparison of the precipitation and circulation patterns that prevailed during the spring and summer of 2010 and 1993, the year of the Great Flood in the American Midwest along the Mississippi and Missouri rivers and their tributaries (e.g. Chagnon 1996).

The heavy precipitation regimes over the US during the spring and summer of 1993 and 2010 exhibited a number of similarities. As described in Chagnon (1996), the evolution of the heavy rainfall pattern over the US during the spring and summer of 1993 was characterized by distinct rainfall regimes, including a build-up phase during April and May and a sustained precipitation phase during July (see Chagnon, 1996 for details). The build-up phase featured localized extreme precipitation events over the central and southern Great Plains, with historically high precipitation totals and flash flooding (similar to what occurred during the spring of 2010). Daily precipitation (mm) for three extreme events during April and May 1993 are shown in Fig. 6. The events in Oklahoma City (April 29, 1993), Northern Texas (May 9, 1993) and Southern Oklahoma (May 10, 1993), ranked second, first and first in the historical record (1948-present),

respectively. It is worth noting that the build-up phase during 2010 occurred later in the spring than the one during 1993.

The sustained precipitation phase during July 1993 featured more generalized precipitation and flooding covering larger areas for longer periods of time. The sustained precipitation regime during 2010 occurred over portions of the upper Midwest (especially Iowa, Wisconsin and southern Minnesota), but again it occurred later in the summer (July-August) than in 1993. A more in depth analysis of the sustained precipitation phase during the summer of 2010 is needed.

While 1993 and 2010 exhibited similar rainfall regimes during the spring and summer months (albeit with slightly shifts in the annual cycle), the atmospheric circulation patterns that contributed to these conditions were somewhat different. A comparison of key circulation features during June 1993 (Fig. 7a) and June 2010 (Fig. 7b) shows that both periods featured persistent and anomalously strong mid-tropospheric westerly flow across the United States and enhanced low-level southerly flow from the western Gulf of Mexico into the southern Plains. It is important to note that anomalies (not full fields) are shown in Fig. 7, where anomalies are departures from mean monthly values for the period 1971-2000.

The pattern in June 1993 featured a western trough and eastern ridge, with a quasi-stationary frontal boundary in between. This frontal boundary, combined with sustained moisture transport form the Gulf of Mexico, provided the focusing mechanism for synoptic-scale upward motion and the extended period of excessive rainfall and flooding in the Midwest (Bell and Janowiak 1995). This pattern was dramatically different from the one that occurred during the buildup phase (April-May 1993), which featured a strong Pacific trough and a ridge to the east in western North America (Bell and Janowiak 1995) that brought the first series of disturbances and heavy precipitation events to the Midwest.

In June 2010, persistent zonal flow from the western Pacific to the eastern United States was the dominant feature, though the eastern ridge was also apparent. The persistent zonal flow provided a duct for cyclones and mesoscale convective systems to propagate across the central and southern Plains contributing to the extreme rainfall and flash flooding events during June 2010. Given that the spring 2010 events covered relatively small areas for short periods, it is unlikely that recirculation of water from available surface moisture played much of a role; this may have been more of a factor during the general flooding that occurred in 1993 (e.g. Dirmeyer and Brubaker 1999) as well as later in the summer of 2010 in the Midwest.

Bell and Janowiak (1995) concluded that El Niño conditions during spring 1993 helped to set up and maintain a very powerful Pacific jet stream that ultimately provided dynamical support for the late spring and summer precipitation pattern tied to the Midwest floods. The persistent jet helped to maintain a quasi-stationary frontal boundary over the Great Plains, which provided a mechanism for the formation of convective complexes that led to the flooding. A similar mechanism may have been operative for the spring 2010 events. Spring 2010 was also characterized by weakening El Niño conditions (the period MJJ 2009 – MAM 2010 qualified as an El Niño episode). This observation suggests that a careful consideration of relationships between the ENSO cycle and precipitation extremes, especially during the spring transition, may be warranted.

## 6. Relationship to the ENSO Cycle

The results in section 5 suggest that shifts in the frequency of daily precipitation extremes over the central United States during the spring and summer months may be tied to the phase of ENSO. This was examined systematically by ranking daily precipitation events at each grid

point by month for the period 1948-2009. The top 50 events were selected and sorted based on whether they occurred during El Nino, La Nina or ENSO neutral conditions. Finally, the monthly results were combined into seasons to obtain the average percentage of top 50 daily precipitation events by ENSO phase (Fig. 8). A classification of historical warm (El Niño) and cold (La Niña) episodes developed by the CPC was used to determine the ENSO phase. El Niño and La Niña episodes were identified using the Oceanic Niño Index or ONI (Kousky and Higgins 2007). The ONI index can be found on the CPC website http://www.cpc.ncep.noaa.gov/products/analysis_monitoring/ensostuff/ensoyears.shtml. The number of El Niño events in the composites are 16, 14, 16, and 20 for JFM, AMJ, JAS and OND; the number of La Niña events in the composites are 21, 17, 18, and 22 for JFM, AMJ, JAS, OND. Thus, the distribution is roughly divided into thirds between El Niño, La Niña and neutral years, and one can use this to get an indication of where there are signals (Fig. 8). Note that only the results for El Niño and La Niña are shown in Fig. 8.

During El Niño a large fraction of extremes occurs along the southern tier-of-states during the fall and winter months consistent with the wetter-than-normal conditions often experienced in those regions. However, there is little or no signal during the spring and summer months. During La Niña a large fraction of extremes occurs in the Pacific Northwest and Ohio Valley during the fall and winter months, again where wetter-than-normal conditions typically occur. Again there is not much of a signal during the spring and summer months. During ENSO neutral years (not shown), the signal is also generally quite weak throughout the annual cycle. Overall, these results suggest that extreme daily events during spring and summer are not heavily influenced by the phase of the ENSO cycle. There could be significant case-to-case variability

within the composites, including during the spring and summer months, but this was not examined.

## 7. Trends

The gridded OI precipitation analysis was used to examine the number of daily precipitation events at various thresholds (including extreme events) that occurred during the period 1948-2009 over the CONUS. The year 2010 was not included because the analysis was carried out mid-way through 2010. For each day in the time series, we counted the number of grid points within CONUS at which the total precipitation exceeded the thresholds 25, 50, 75, 100, and 125mm. A plot of the time series (365-d running mean) of the number of events for the thresholds of 25 mm, 50 mm, 75 mm, 100 mm, and 125 mm is shown in Fig. 9.

The results show several interesting features. Each of the time series has large interannual variability, with good agreement between El Niño (La Niña) and increases (decreases) in the number of daily events especially at the higher thresholds (100 mm and 125 mm). There is little obvious evidence of trends at lower thresholds, but some indication of increased variability and increases in the number of extremes at the higher thresholds, particularly after 1980. No attempt was made to systematically compare these results to recent assessment reports, such as the USGCRP (2009) which reported clear trends in the United States towards increasing frequency (and intensity) of heavy downpours (top 1% of events) over the period 1958-2007. We note that an examination of the number of daily precipitation events at various thresholds that occurred during the period 1948-2009 over CONUS, but by season (i.e. JFM, AMJ, JAS, OND) also did not reveal any obvious trends, though again there was a good correspondence, especially during the fall and winter seasons when ENSO influences on storminess are the strongest. The extent

to which any changes in variability might be due to changes in station counts versus a stronger connection between ENSO and extremes has not been investigated.

We also examined counts of the number of very heavy precipitation events in the more recent period (1979-2009) and in the earlier period (1948-1978), in particular to see if there were any obvious signals in daily precipitation extremes over the central US during the spring and summer months in the more recent period. For this we ranked the daily precipitation values (1948-2009) for each month at all grid points in CONUS. We took the top 50 values (roughly the 97th percentile or greater) and counted the number of events that occurred during the period 1948-1978 (31 years) versus during the period 1979-2009 (31 years). Counts (out of a possible total of 50 events at each location) for 1979-2009 for each month are shown in Fig. 10. Areas where the count is larger than 27 of 50 events are shaded in greens and areas where the count is less than 23 of 50 events are shaded in browns.

Some notable increases for the recent period are evident over portions of the southern tier-of-states and the south central United States during fall and winter (Fig. 10). The patterns appear to be ENSO-like, which may indicate that the strong El Nino episodes (1982/83, 1991/92 and 1997/98) help to explain the increase in heavy precipitation events. Focusing on the central United States, there does not appear to be a spatially coherent change (increase or decrease) in the number of extreme daily events during the spring and summer months.

Table 2 shows the percentage of top 50 extreme events that occurred during 1948-1978 and during 1979-2009 for CONUS as well as the percent difference between the 2 periods. For the CONUS, there have been 3.4% more daily extreme events during 1979-2009 than during 1948-1978. Although there are more events in the more recent period in every month of the year, the largest increases are during autumn and late winter, consistent with ENSO. A 4.4% increase in

daily precipitation extremes occurred during May, though these increases appear to have occurred primarily in the Southwest and Ohio Valley (Fig. 10).

Overall, the results in Fig. 10 and Table 2 are qualitatively consistent with recent assessment reports (e.g. USGCRP 2009) that have reported increases in the amounts of precipitation falling in very heavy precipitation events and a trend towards more very heavy precipitation for the nation as a whole. No attempt has been made to look at increases in the number of cases on a regional or local basis, although the data are available.

**8. Summary and Future Plans**

The spring of 2010 was characterized by a large number of heavy rain events leading to major flooding across portions of the central and southern United States. Each of the 2010 major flood events was associated with historic rainfall totals. While there were circulation features in common to several of the cases, a unique combination of synoptic-scale and mesoscale circulation features came together to define each case. While moist air masses, emanating from the Gulf of Mexico were present in each case, the precipitable water values were not at record levels when compared to some recent land falling tropical cyclones. However, all five of the cases examined here were associated with moisture plumes that extended deep into the Caribbean, and exhibited the characteristics of the "Maya Express" flood events (Dirmeyer and Kinter 2009) that link tropical moisture from the Caribbean and Gulf of Mexico to mid-latitude flooding over North America.

The heavy precipitation regimes over the US during the spring and summer of 1993 and 2010 exhibited a number of similarities, including build-up and sustained phases. Additional

comparisons to sort out the extent of these similarities, including comparisons to other wet years over the central United States, are needed.

This analysis showed a 3.4% increase in extreme events during the period 1979-2009 compared to the period 1948-1978, when averaged over CONUS. Extreme events increased in every month of the year, with notable increases in October, November and March (i.e. during the transition periods in the annual cycle).

According to the USGCRP (2009) assessment report, much of the increase in the amount of rain falling in the heaviest downpours has occurred since 1970, during a period in which average temperatures in the U.S. have increased by approximately 1°F (e.g. IPCC 2007). The IPCC (2007) report also concludes that water vapor in the global atmosphere has increased by about 4% since 1970. Trenberth et al. (2005) used satellite measurements to document a 1.3% per decade increase in water vapor over the global oceans since 1988. Although one cannot attribute a single event (or even series of events over a season) to climate change, it is logical to conclude that a systematic increase in water vapor in the atmosphere could have a systematic influence on extreme precipitation events by invigorating storms and by providing additional moisture for heavy rainfall. While we cannot conclude that the spring 2010 heavy precipitation events were a consequence of global warming, it is logical to suggest that the events were enhanced by the presence of significant water vapor anomalies in the atmosphere as shown here. Moreover, it is logical to conclude that we can expect an increase in heavy precipitation events and the associated flooding in the United States (and worldwide) if the climate continues to warm.

Additional studies of daily precipitation extremes are planned to support the findings reported here and to improve our understanding of the linkage between precipitation extremes, climate variability and climate change. This includes studies of the relative contributions of

diurnal, daily, interannual and decadal variability in daily precipitation to the total variability, of the uncertainties due to changes in instrumentation and changes in the number of observations through the historical record, and of the ability of climate models (such as the NCEP climate forecast System) to reproduce the statistics of daily precipitation extremes found in nature.

## 9.0 Acknowledgments

The authors gratefully acknowledge the assistance of Dr. Soo-Hyun Yoo of NOAA/CPC who provided considerable assistance with the analysis for this project. The authors also thank Dr. Wei Shi and Jon Gottschalck, who provided constructive reviews of early versions of this manuscript.

## 10.0 References

Bell, G.D., and J.E. Janowiak, 1995: Atmospheric circulation associated with the Midwest floods of 1993. *Bull. Amer. Met. Soc*., **76**, 681-696.

Chagnon, S., 1996: *The Great Flood of 1993: Causes, Impacts, And Responses,* Westview, 1996, 321 pp. ISBN 0813326192,

Chen, M., W. Shi, P. Xie, V. B. S. Silva, V E. Kousky, R. W. Higgins, and J. E. Janowiak, 2008: Assessing objective techniques for gauge-based analyses of global daily precipitation, *J. Geophys. Res*., **113**, D04110, doi:10.1029/2007JD009132.

Dirmeyer, P. A., and J. L. Kinter III, 2009: The Maya Express - Late spring floods in the US Midwest. *Eos – Transactions of the American Geophysical Union*, **90**, 101-102.

Dirmeyer, P. A., and K. L. Brubaker, 1999: Contrasting evaporative moisture sources during the drought of 1988 and the flood of 1993. *J. Geophys. Res.*, **104**, 19383-19397.

Higgins, R.W., W. Shi, E. Yarosh, and R. Joyce, 2000: Improved United States precipitation quality control system and analysis. NCEP/Climate Prediction Center ATLAS No. 7, 40 pp. [http://www.cpc.ncep.noaa.gov/research_papers/ncep_cpc_atlas/7/index.html]

IPCC, 2007: "Summary for Policymakers" (PDF). *Climate Change 2007: The Physical Science Basis. Contribution of Working Group I to the Fourth Assessment Report of the Intergovernmental Panel on Climate Change*. http://www.ipcc.ch/pdf/assessment-report/ar4/wg1/ar4-wg1-spm.pdf.

Kalnay E., and co-authors, 1996: The NCEP/NCAR 40-year reanalysis project. *Bull. Amer. Met Soc.* **77**, 437-471.

Kousky, V. E. and R. W. Higgins, 2007: An Alert Classifications System for monitoring and assessment of the ENSO cycle, *Weather and Forecasting*, **Vol. 22, No. 2**,353–371.

Nielsen-Gammon, Zhang, Odins and Myoung, 2005: Extreme rainfall patterns in Texas: Patterns and predictability. Physical Geography, 2005, 26, 5, pp. 340-364. Copyright 2005 by V. H. Winston & Son, Inc.

Trenberth, K.E., J. Fasullo, and L. Smith, 2005: "Trends and variability in column-integrated atmospheric water vapor", *Climate Dynamics,* **24**, 741-758.

U.S. Global Change Research Program, 2009. *Global Climate Change Impacts in the United States*, T.R. Karl, J.M. Melillo, and T.C. Peterson, (eds.). Cambridge University Press, 191 pp.

## 11.0 Table Captions

**Table 1.** Dates, daily rainfall amounts, and historical ranking for five extreme daily precipitation events during May and June 2010.

**Table 2.** Percentage of the number of top 50 daily precipitation events that occurred during the period 1948-1978 and during the period 1979-2009 for the continental United States.

## 12.0 Figure Captions

**Figure 1.** Daily precipitation (mm) for selected extreme events during spring 2010: (a) May 3, 2010, (b) June 10, 2010, (c) June 11, 2010, (d) June 13, 2010 and (e) June 15, 2010.

**Figure 2.** Daily precipitation percentiles for days corresponding to the daily extremes in Fig. 1: (a) May 3$^{rd}$ for the grid box surrounding Nashville, Tennessee, (b) June 10$^{th}$ for the grid box with maximum precipitation over eastern Texas, (c) June 11$^{th}$ for the grid box with maximum precipitation over western Arkansas, (d) June 13$^{th}$ for the grid box with maximum precipitation over South Central Kansas and (e) June 15$^{th}$ for the grid box with maximum precipitation over Central Oklahoma. For (a)-(e), the daily extreme was ranked the highest in the period of record (1948-2010) (see Table 1).

**Figure 3.** Estimates of the extreme maximum daily precipitation (mm) that might be expected to occur given a sufficiently long historical record. See text for the procedure used to estimate the upper bounds on daily precipitation extremes.

**Figure 4.** Top Row: 500-hPa height (dam), 500-hPa vector wind (m s$^{-1}$) and 500-hPa isotachs of wind speed (m s$^{-1}$) for selected extreme events during spring 2010. Bottom Row: 925-hPa vector wind (m s$^{-1}$) and 925-hPa isotachs of wind speed (m s$^{-1}$) for selected extreme events during spring 2010. Dates of the extreme events are indicated across the top of the figure. Isotachs are shaded as indicated by the color bars.

**Figure 5.** Precipitable water (mm) for selected extreme events during spring 2010. Dates of the extreme events are indicated across the top of the figure.

**Figure 6.** Daily precipitation (mm) for selected extreme events during April and May 1993: (a) April 29, 1993, (b) May 9, 1993, (c) May 10, 1993.

**Figure 7.** Top: 500-hPa height anomalies (dam), 500-hPa vector wind anomalies (m/s) and 500-hPa isotachs of anomalous wind speed (m $s^{-1}$) for June 1993 and June 2010. Bottom: 925-hPa vector wind anomalies (m/s) and 925-hPa isotachs of anomalous wind speed (m $s^{-1}$) for June 1993 and June 2010. Anomalies are departures from mean monthly values for the period 1971-2000. Isotachs are shaded as indicated by the color bars.

**Figure 8.** Fraction (in percent) of the top 50 daily precipitation events occurring during El Niño and La Niña. Results are shown by season and are based on the period 1948-2009. The number of El Niño events is 16, 14, 16, and 20 for JFM, AMJ, JAS and OND. The number of La Niña events is 21, 17, 18 and 22 for JFM, AMJ, JAS and OND. See text for details on the method used to obtain the composites.

**Figure 9.** Number of daily precipitation events exceeding thresholds of 25 mm, 50 mm, 75 mm, 100 mm, and 125 mm for the continental United States. A 365-day running mean of the results is shown.

**Figure 10.** Number of top 50 daily precipitation events that occurred during 1979-2009. Areas shaded in greens and blues had more events in the recent period (1979-2009) than in the earlier period (1948-1978). See text for details on the ranking procedure.

| Event | Date | Daily Rainfall (mm) | Historical Ranking for the Date (based on 1948-present) |
|---|---|---|---|
| **Nashville, TN** | May 3, 2010 | 184.0 | 1 |
| **Eastern Texas** | June 10, 2010 | 216.4 | 1 |
| **Western Arkansas** | June 11, 2010 | 103.4 | 1 |
| **South-Central Kansas** | June 13, 2010 | 167.5 | 1 |
| **Central Oklahoma** | June 15, 2010 | 147.0 | 1 |

**Table 1.** Dates, daily rainfall amounts, and historical ranking for five extreme daily precipitation events during May and June 2010.

| | Jan | Feb | Mar | Apr | May | Jun | Jul | Aug | Sep | Oct | Nov | Dec | Ave |
|---|---|---|---|---|---|---|---|---|---|---|---|---|---|
| **1) 1948-1978** | 49.8 | 48.8 | 46.1 | 49.9 | 47.8 | 49.6 | 47.7 | 49.3 | 49.3 | 45.6 | 46.5 | 49.3 | 48.3 |
| **2) 1979-2009** | 50.2 | 51.2 | 53.9 | 50.0 | 52.2 | 50.3 | 52.2 | 50.7 | 50.7 | 54.4 | 53.5 | 50.7 | 51.7 |
| **Diff. 2)-1)** | 0.4 | 2.5 | 7.8 | 0.1 | 4.4 | 0.7 | 4.5 | 1.4 | 1.4 | 8.9 | 7.0 | 1.3 | 3.4 |

**Table 2.** Percentage of the number of top 50 daily precipitation events that occurred during the period 1948-1978 and during the period 1979-2009 for the continental United States.

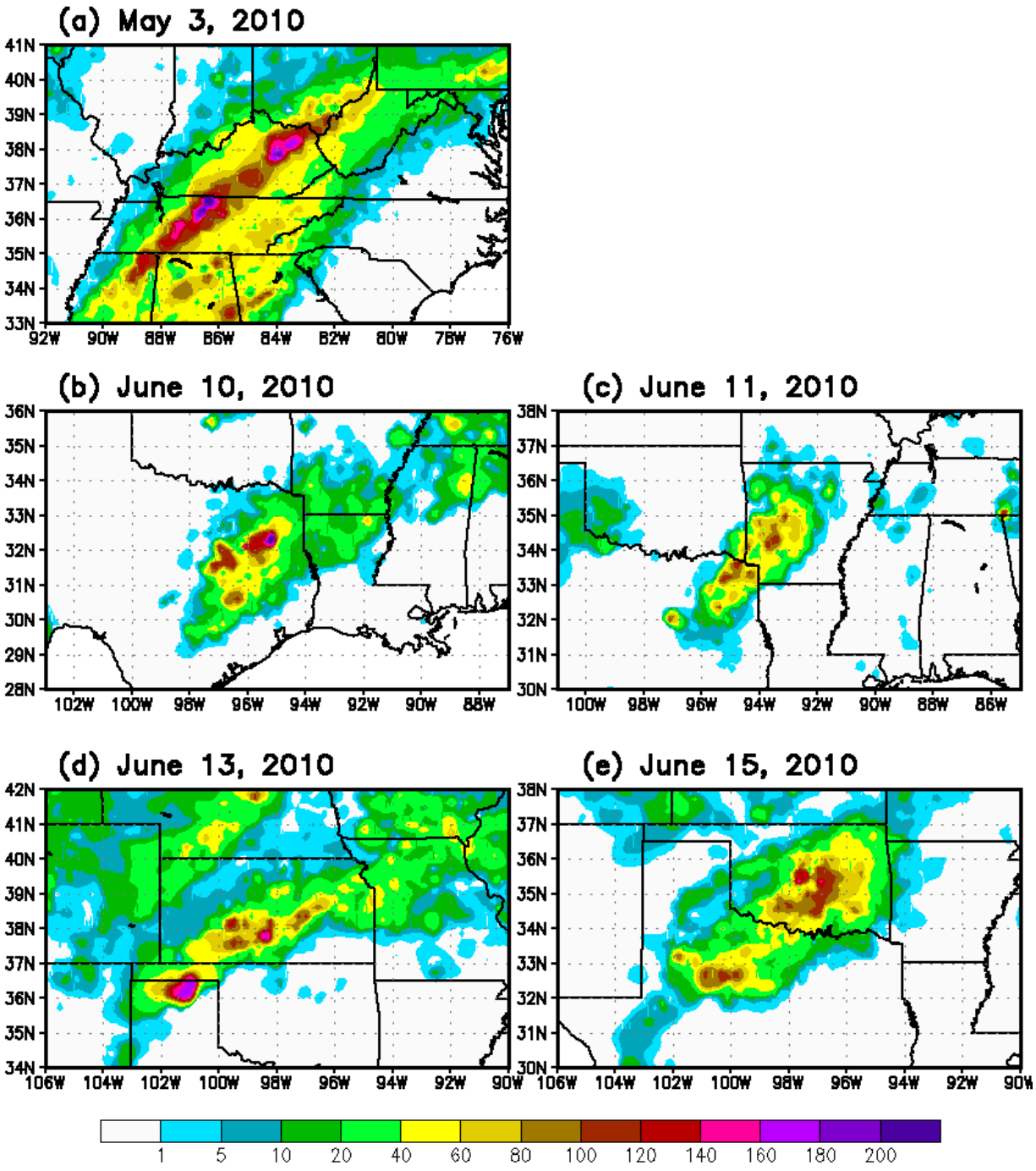


**Figure 1.** Daily precipitation (mm) for selected extreme events during spring 2010: (a) May 3, 2010, (b) June 10, 2010, (c) June 11, 2010, (d) June 13, 2010 and (e) June 15, 2010.

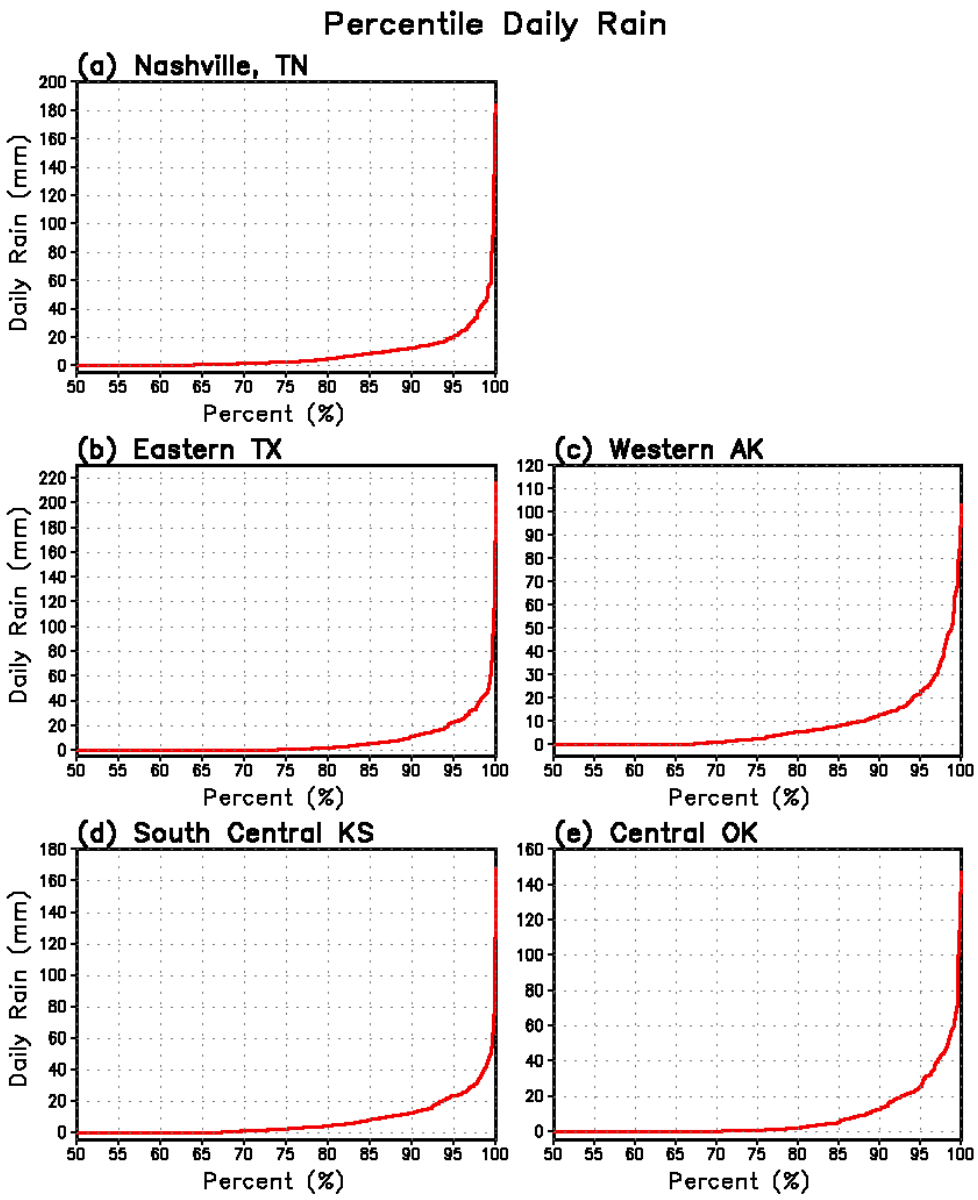


**Figure 2.** Daily precipitation percentiles for days corresponding to the daily extremes in Fig. 1: (a) May 3rd for the grid box surrounding Nashville, Tennessee, (b) June 10th for the grid box with maximum precipitation over eastern Texas, (c) June 11th for the grid box with maximum precipitation over western Arkansas, (d) June 13th for the grid box with maximum precipitation over South Central Kansas and (e) June 15th for the grid box with maximum precipitation over Central Oklahoma. For (a)-(e), the daily extreme was ranked the highest in the period of record (1948-2010) (see Table 1).

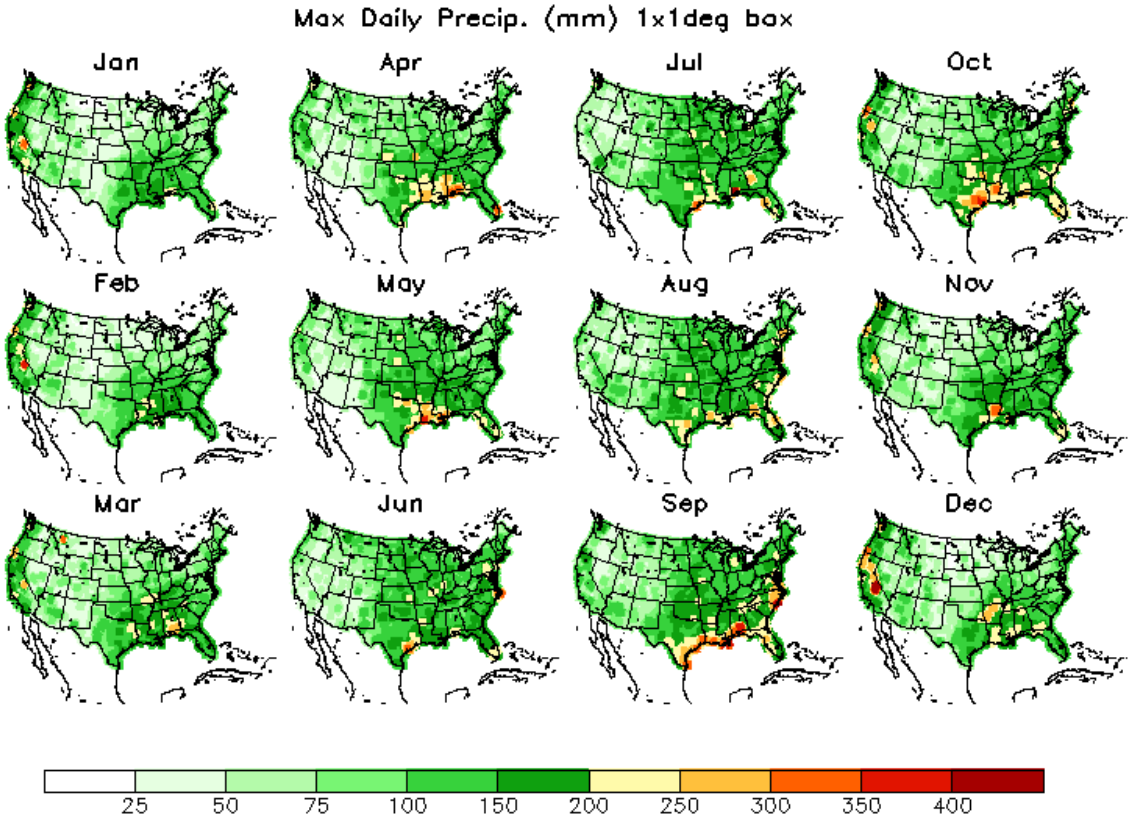


**Figure 3.** Estimates of the extreme maximum daily precipitation (mm) that might be expected to occur given a sufficiently long historical record. See text for the procedure used to estimate the upper bounds on daily precipitation extremes.

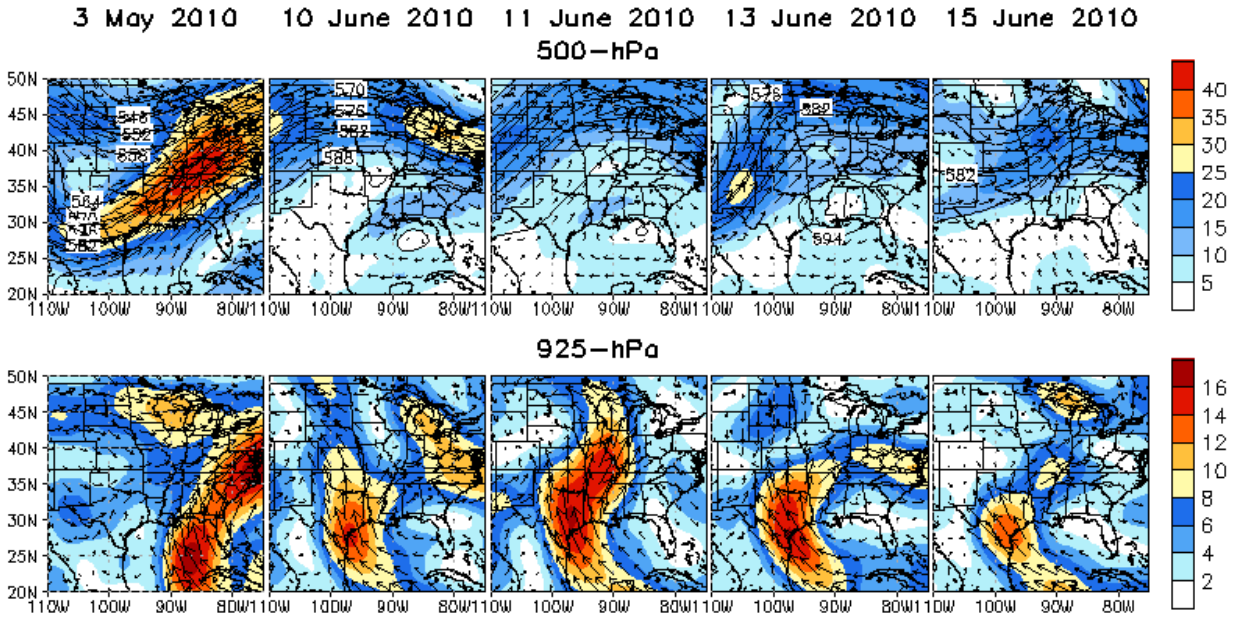


**Figure 4.** Top Row: 500-hPa height (dam), 500-hPa vector wind (m $s^{-1}$) and 500-hPa isotachs of wind speed (m $s^{-1}$) for selected extreme events during spring 2010. Bottom Row: 925-hPa vector wind (m $s^{-1}$) and 925-hPa isotachs of wind speed (m $s^{-1}$) for selected extreme events during spring 2010. Dates of the extreme events are indicated across the top of the figure. Isotachs are shaded as indicated by the color bars.

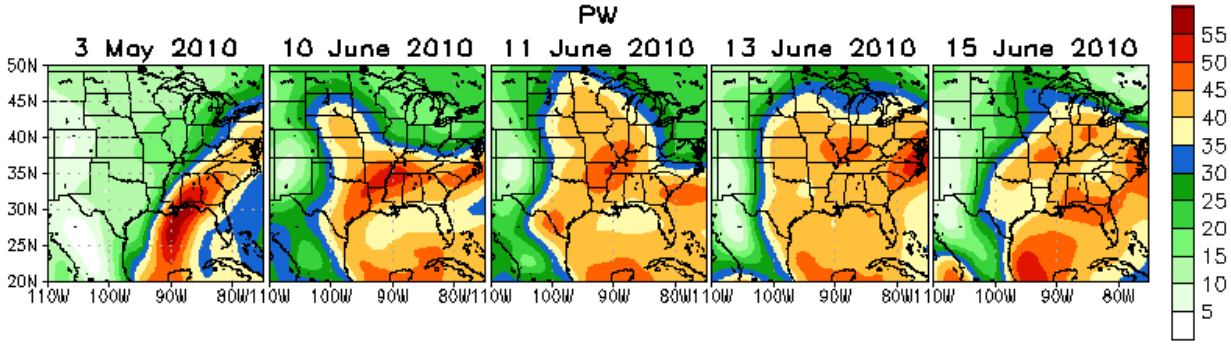


**Figure 5.** Precipitable water (mm) for selected extreme events during spring 2010. Dates of the extreme events are indicated across the top of the figure.

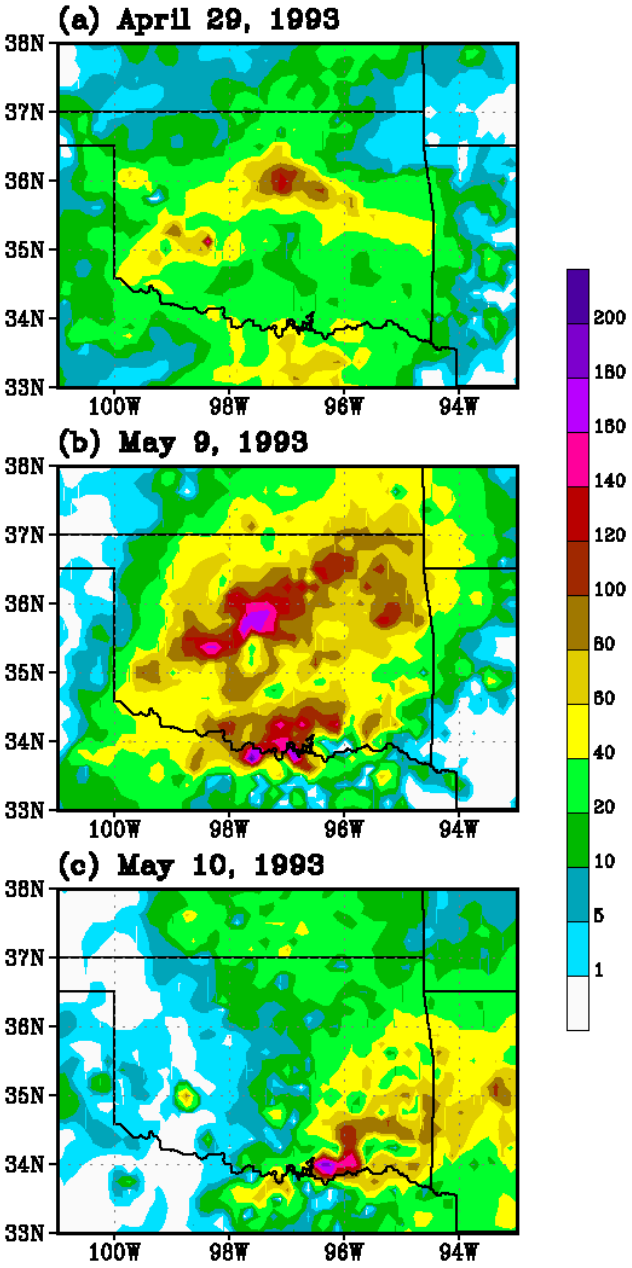


**Figure 6.** Daily precipitation (mm) for selected extreme events during April and May 1993: (a) April 29, 1993, (b) May 9, 1993, (c) May 10, 1993.

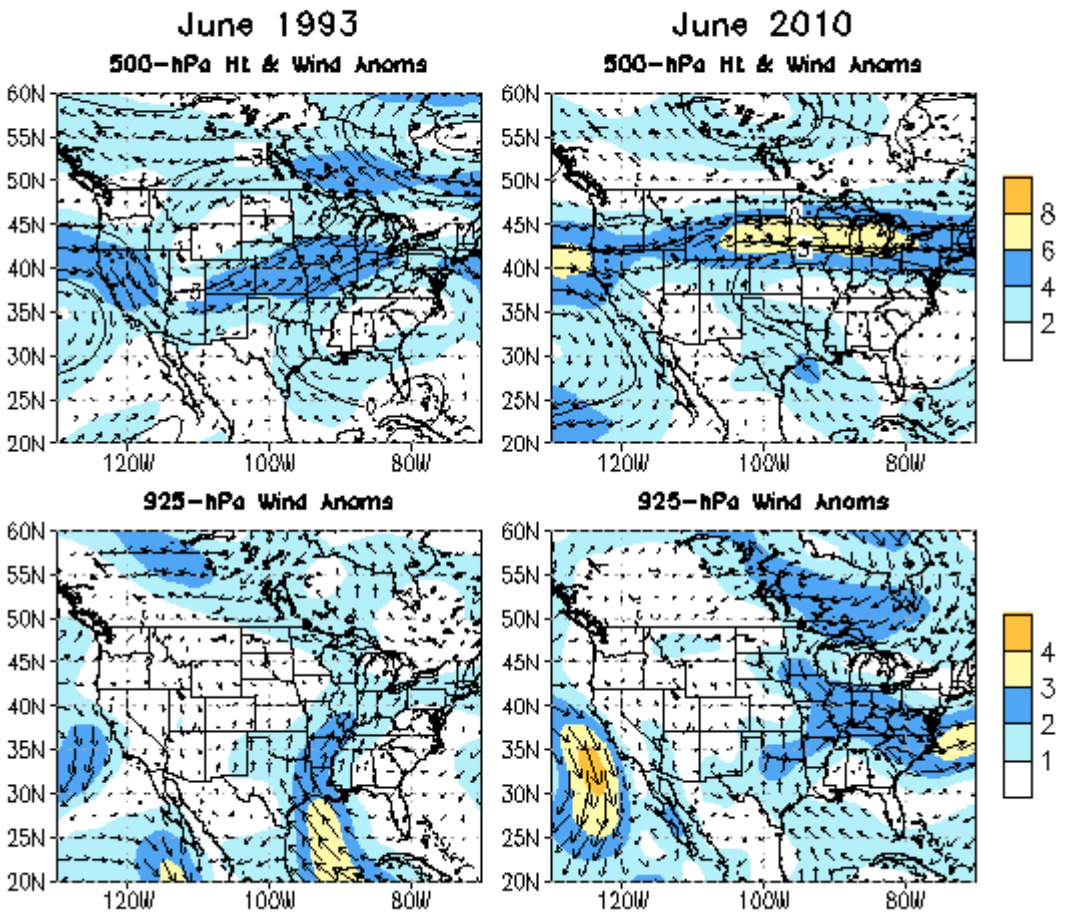


**Figure 7.** Top: 500-hPa height anomalies (dam), 500-hPa vector wind anomalies (m/s) and 500-hPa isotachs of anomalous wind speed (m $s^{-1}$) for June 1993 and June 2010. Bottom: 925-hPa vector wind anomalies (m/s) and 925-hPa isotachs of anomalous wind speed (m $s^{-1}$) for June 1993 and June 2010. Anomalies are departures from mean monthly values for the period 1971-2000. Isotachs are shaded as indicated by the color bars.

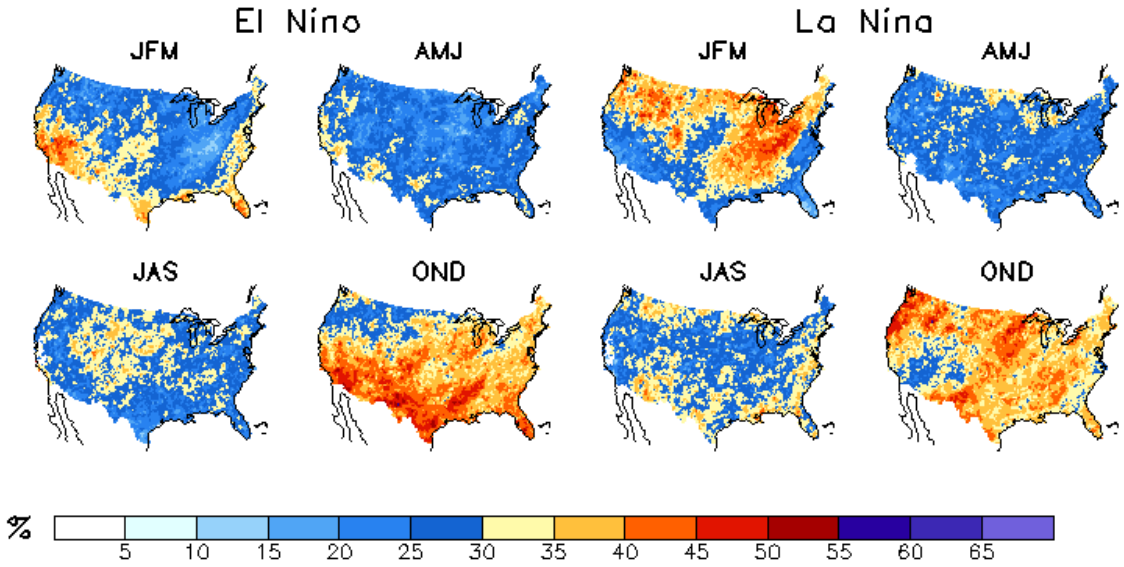


**Figure 8.** Fraction (in percent) of the top 50 daily precipitation events occurring during El Niño and La Niña. Results are shown by season and are based on the period 1948-2009. The number of El Niño events is 16, 14, 16, and 20 for JFM, AMJ, JAS and OND. The number of La Niña events is 21, 17, 18 and 22 for JFM, AMJ, JAS and OND. See text for details on the method used to obtain the composites.

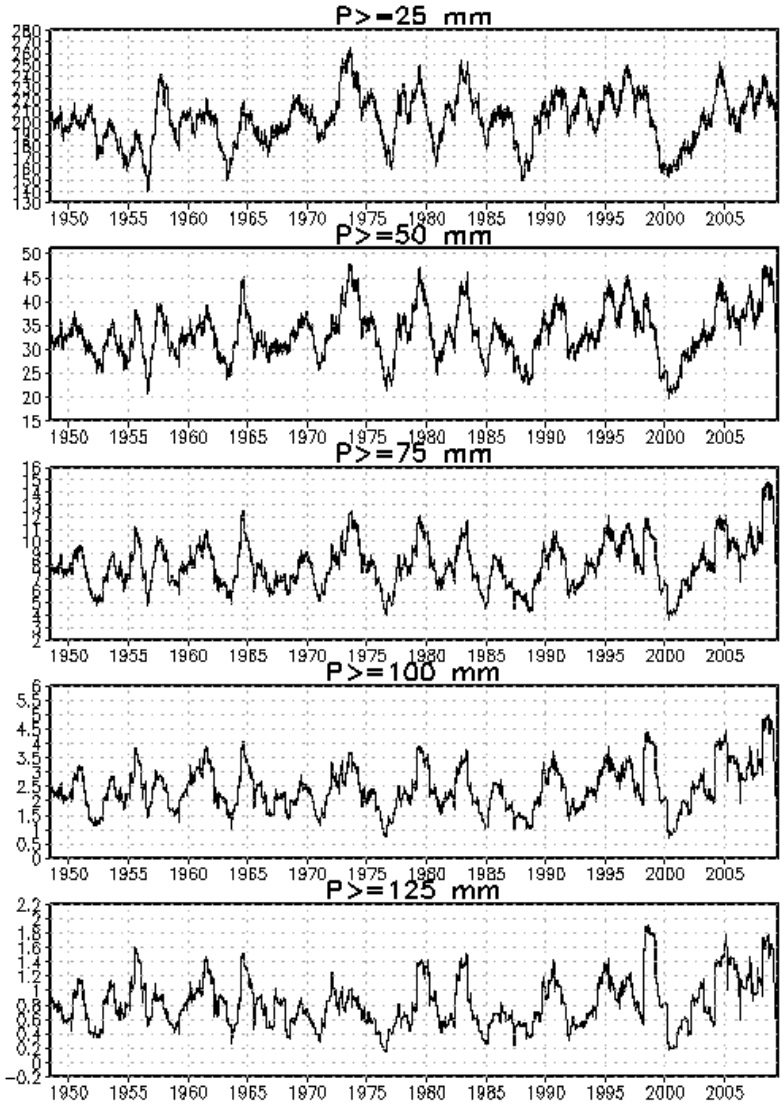


**Figure 9.** Number of daily precipitation events exceeding thresholds of 25 mm, 50 mm, 75 mm, 100 mm, and 125 mm for the continental United States. A 365-day running mean of the results is shown.

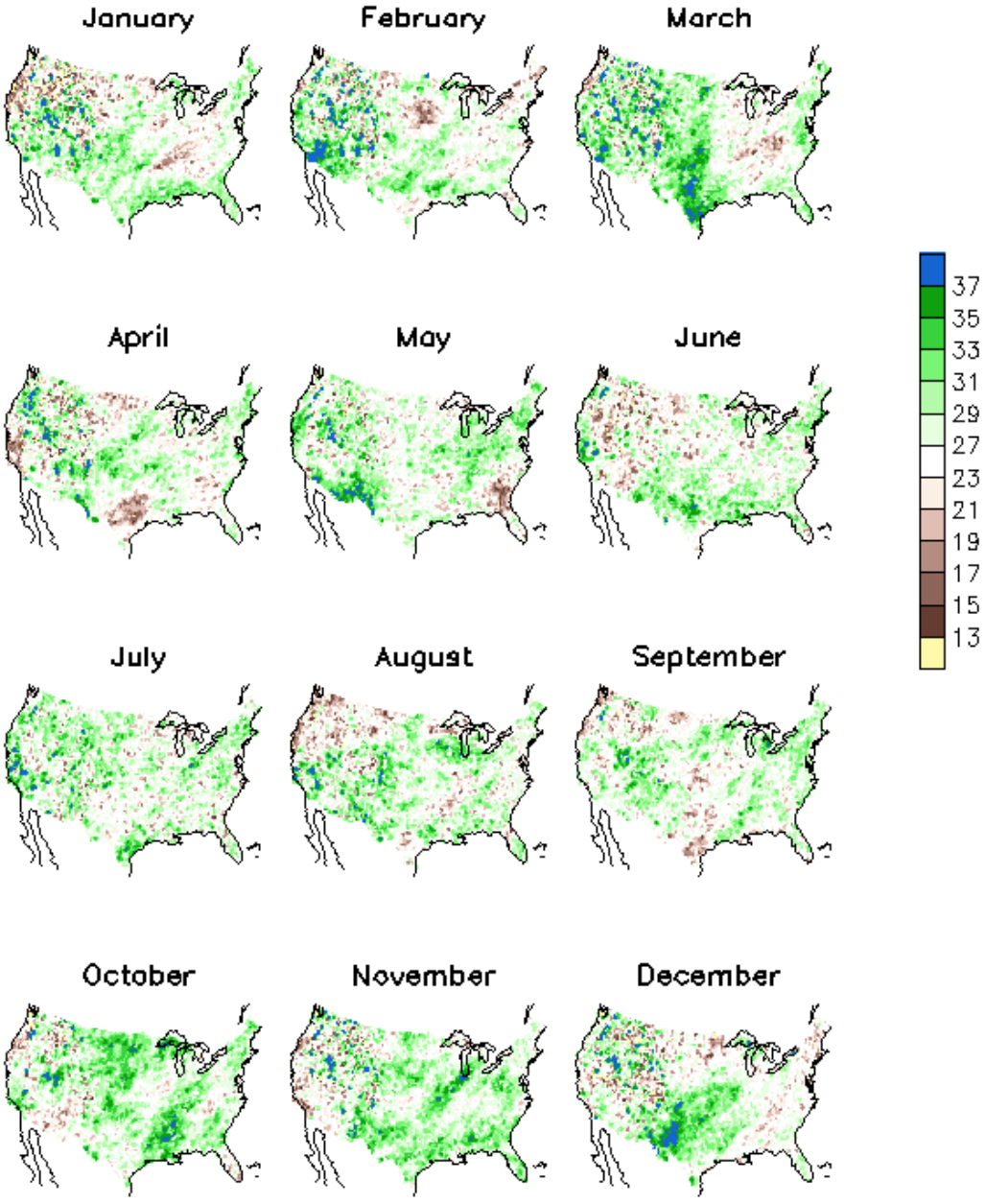


**Figure 10.** Number of top 50 daily precipitation events that occurred during 1979-2009. Areas shaded in greens and blues had more events in the recent period (1979-2009) than in the earlier period (1948-1978). See text for details on the ranking procedure.